

INJECTION EFFICIENCY IN HYBRID IRCCD'S

A. J. Steckl

Electronics Research Division
Rockwell International Corporation
Anaheim, California 92803

12:03 — 12:20 possible

ABSTRACT. In this paper an equivalent circuit approach is used to model the direct injection hybrid IRCCD. The injection efficiency is calculated as a function of frequency up to 10 MHz for different values of detector and CCD input circuit parameters. The dynamic effect of the total detector current on the injection efficiency is taken into account by a first-order correction. For a typical case, a photodiode with a resistance of $5K \Omega$, a capacitance of 20pF and CCD input transconductance of $500 \mu\text{mho}$ and an input capacitance of 1pF, an injection efficiency of $\sim 67\%$ is calculated at the minimum read frequency of 1.34 MHz.

I. INTRODUCTION

In the direct injection IRCCD, the photo-generated charge is directly introduced into the CCD shift register [1-5]. Since this is in effect a DC coupled system, only IR detectors which exhibit relatively small DC currents (e.g. photovoltaic, extrinsic detectors) can be coupled to the CCD due to the latter's limited charge handling capacity. A critical parameter of the direct injection IRCCD is the injection efficiency, defined as the ratio of the charge introduced into the CCD to the total charge generated by the detector. In this paper, the frequency dependence of the injection efficiency is examined as a function of the detector and CCD input parameters. Since different IR focal plane scanning organizations (e.g. star-ring, parallel, serial) operate at different rates (from 30 Hz to 6 MHz) it becomes very important to be able to predict the injection efficiency at the appropriate frequency in order to calculate the overall performance of the IRCCD.

The basic direct injection concept is illustrated for a hybrid IRCCD consisting of a (Pb,Sn) Te photo-diode and an n-channel CCD (see Fig. 1). The (Pb,Sn) Te/PbTe heterostructure [6] is particularly attractive for a hybrid IRCCD array since integration can be achieved in a

relatively simple sandwich structure with full use of the detector active area and requiring no interconnects (see Fig. 2). As shown in Fig. 1, the IR diode is connected in parallel to a silicon diode which serves as an input tap to the CCD. The first MOS gate, V_G , serves to reverse bias both diodes. While the charge accumulates under the storage gate V_S , it is isolated from the CCD channel by the transfer gate V_T . After one read time, t_R , V_T is biased into inversion and the accumulated charge is transferred into the CCD channel.

II. EQUIVALENT CIRCUIT MODEL

To evaluate the direct injection efficiency, the equivalent load presented to the detector by the CCD is first considered. The CCD input stage is effectively a MOSFET with the input diffusion representing the source and the potential, ϕ_S , of the inverted surface under the V_S electrode, representing the drain. Since we want the charge to accumulate under the storage electrode, we need $V_S > V_G$, thus driving the MOSFET into saturation. However, the saturated drain current is not free to take the value it normally would in the grounded source MOSFET configuration since it is driven by the detector current. This results in an increase in the source potential required

to satisfy the appropriate current flow. Under these conditions the gate and drain voltages must be referred to this effective source potential. Since we are in the saturation region, the drain conductance $g_D = \frac{\partial I_D}{\partial V_D} = 0$ and the input conductance seen by the detector is given by the variation of the drain current with changes in the gate-to-source voltage, V_{GS} , or the transconductance g_M . It should be pointed out, however, that as charge accumulates under V_{GS} , the surface potential decreases to the point where the drain-to-source potential is lower than the gate-to-source potential thus forcing the MOSFET out of the saturation regime. As the drain-to-source potential decreases further the drain current will decrease accordingly, resulting in a potentially very useful self-limiting action. The CCD input capacitance is the parallel combination of the source diode capacitance, channel capacitance and gate-to-source capacitance with the latter being the dominating factor [8].

The equivalent circuit for the detector/CCD input circuit can thus be simply shown as in Figure 3, where i_D is the detector current (signal + background + dark current) and G_D and C_D are the detector conductance and capacitance. The current flow in the circuit is then given by

$$i_D = i_1 + i_2 \quad (1)$$

$$i_1 [G_D + sC_D]^{-1} = i_2 [g_m + sC_{gs}]^{-1} \quad (2)$$

where i_2 is the current injected into the CCD. The injection efficiency, η_{INJ} , defined as the ratio of the current flowing into the CCD over the total detector current, can then be obtained from Equations (1) and (2):

$$\eta_{INJ} = \frac{i_2}{i_D} = \frac{g_m}{g_m + G_D} \frac{A}{\left[1 + \omega^2 \left(\frac{C_D + C_{gs}}{G_D + g_m}\right)^2\right]} \quad (3)$$

where A is given by:

$$A = \sqrt{1 + \omega^2 \frac{2C_{gs}^2 \left(1 + \frac{G_D}{g_m}\right) + \frac{1}{g_m^2} [C_{gs}^2 G_D^2 + g_m^2 C_D^2 + [(C_{gs} + C_D)^2 C_{gs}^2 \omega^2]]}{(G_D + g_m)^2}} \quad (4)$$

In the two frequency limits the injection efficiency simplifies to the expected resistance and capacitance divider network:

$$\omega \rightarrow 0 \quad \eta_{INJ} = \frac{g_m}{g_m + G_D} \quad (5)$$

$$\omega \rightarrow \infty \quad \eta_{INJ} = \frac{C_{gs}}{C_D + C_{gs}} \quad (6)$$

In addition, for reasonably good photo-diode characteristics, the injection efficiency is well approximated in the submegahertz range by

$$\omega \leq 1 \text{ MHz} \quad \eta_{INJ} = \frac{\eta_{INJ}(0)}{\left[1 + \omega^2 \left(\frac{C_D + C_{gs}}{g_m + G_D}\right)^2\right]} \quad (7)$$

where $\eta_{INJ}(0)$ is defined by Equation (5).

III. HYBRID IRCCD PARAMETERS

For a (Pb,Sn) Te/PbTe diode sensitive over the entire 8-12 μm region, the background photon flux is roughly 1×10^{17} photons/cm²-sec which for an optical area of 5×5 mils² results in a background current of $\sim 2 \mu\text{A}$. The mesa structure of the diode results in an electrical area of the detector smaller than the optical area, giving rise to effective optical gain. The electrical properties of the device are, therefore, a function of the electrical area one can obtain through the mesa etching. Under these conditions the detector parameters vary typically from $1\text{K}\Omega$ to $10\text{K}\Omega$ for R_D and 10 to 100 pF for C_D at an effective reverse bias of the order of 100 mV [6]. The total detector current at this bias is taken to vary from $10 \mu\text{A}$ ($R_D = 10\text{K}\Omega$) to $100 \mu\text{A}$ ($R_D = 1\text{K}\Omega$).

Can be thought of as a current source if input is a virtual ground or current sink!

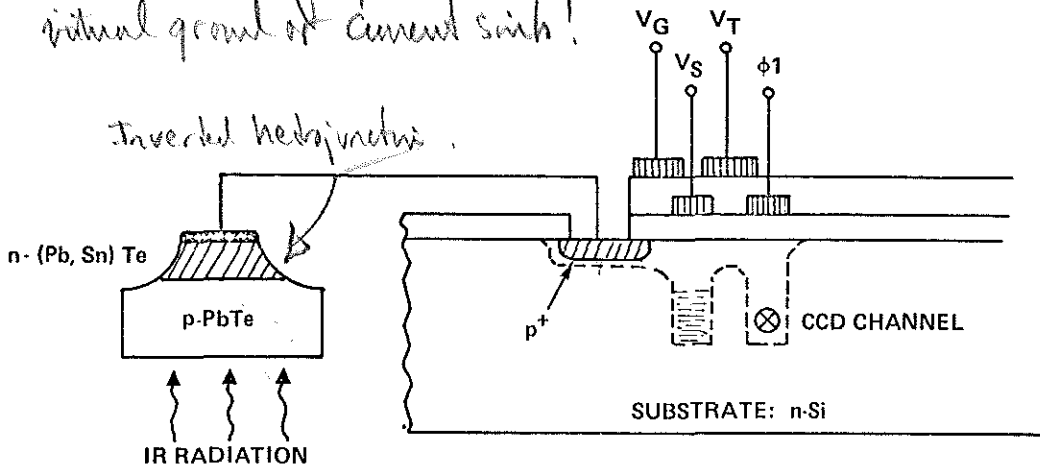


Fig. 1 Hybrid IRCCD: Direct Injection from (Pb,Sn)Te/PbTe Heterodiode.

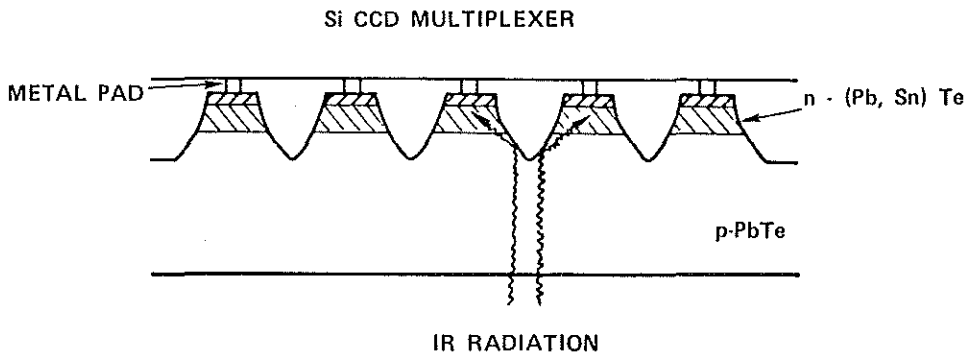


Fig. 2 Hybrid IRCCD Two Chip Device Using Inverted Heterojunction Detector Array.

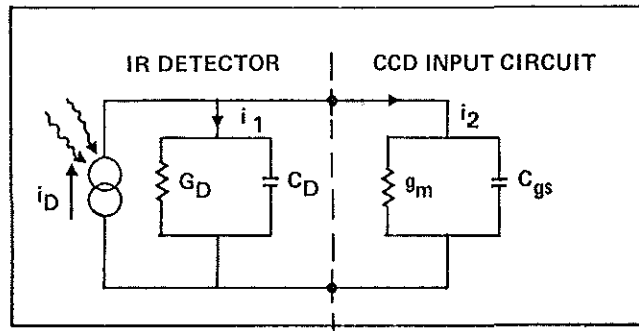


Fig. 3 Direct Injection Equivalent Circuit Model.

5. For a review of IRCCD's and additional references see A. J. Steckl, R. D. Nelson, B. T. French, R. A. Gudmundsen and D. Schecter, "Application of Charge Coupled Devices to IR Detection and Imaging", Proc. IEEE, Vol. 63, p. 50, Jan. 75.
6. A. M. Andrews, J. T. Longo, J. E. Clarke and P. Neuber, "(Pb,Sn) Te Inverted Heterostructure Photodiode", presented at the Device Research Conf., Santa Barbara, CA, June 1974.
7. S. M. Sze, Physics of Semiconductor Devices, J. Wiley, N.Y., 1969.
8. P. Richman, MOS Field-Effect Transistors and Integrated Circuits, J. Wiley, N.Y., 1973.
9. J. Shott and R. Melen, "The Razorback CCD", Digest 1975 I.S.S.C. Conf. Philadelphia, PA, Feb. 75.
10. G. W. Ludwig and R. L. Watters, "Drift and Conductivity Mobility in Silicon", Phys. Rev., Vol. 101, p. 1699, March 15, 1956.

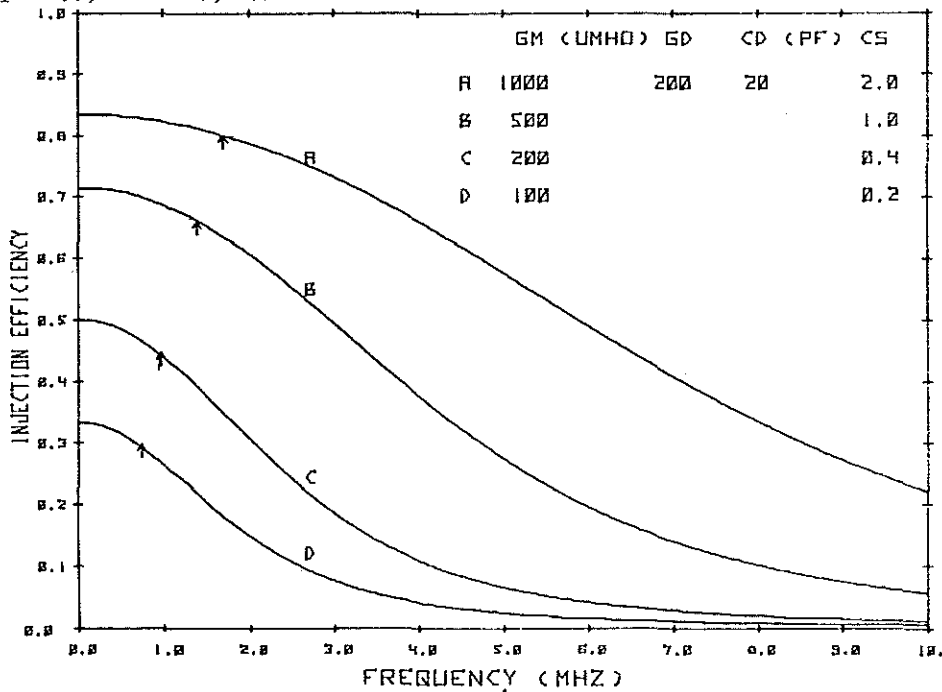


Fig. 4 Injection Efficiency vs. Frequency for Different Values of Input Transconductance and Capacitance

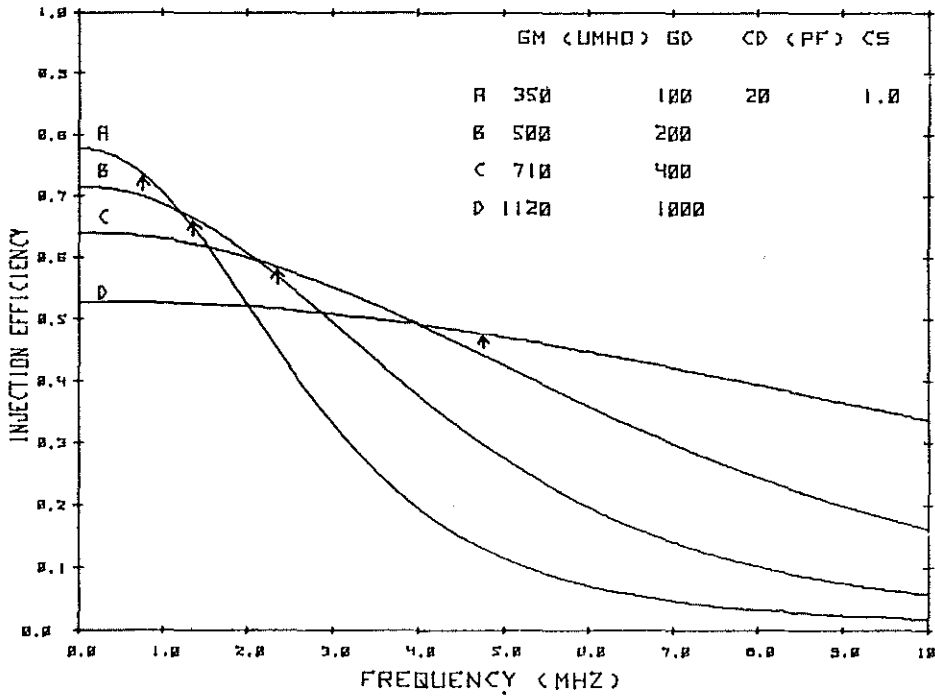


Fig. 5 Injection Efficiency vs. Frequency for Different Values of Detector Conductance

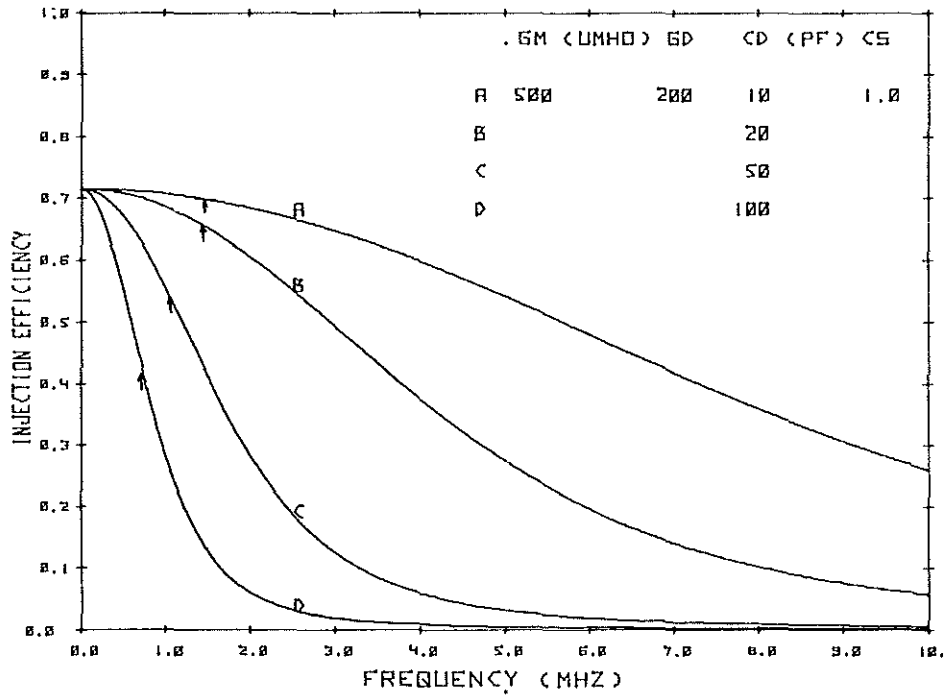


Fig. 6 Injection Efficiency vs. Frequency for Different Values of Detector Capacitance